GSA DATA REPOSITORY 2010167

Small-scale convection at the edge of the Colorado Plateau: Implications for topography, magmatism, and evolution of Proterozoic lithosphere

J.W. van Wijk *(1),W.S. Baldridge (2), J. van Hunen (3), S. Goes (4), R. Aster (5), D.D. Coblentz (2), S.P. Grand (6), J. Ni (7)

*Corresponding author.
(1) Department of Earth and Atmospheric Sciences, University of Houston, 312 Science & Research Bldg. 1, Houston, TX 77204, jwvanwijk@uh.edu
(2) Earth and Environmental Sciences Division, Los Alamos National Laboratory, Los Alamos, NM
(3) Department of Earth Sciences, Durham University, Durham, UK
(4) Department of Earth Science and Engineering, Imperial College, London, UK
(5) Department of Earth and Environmental Science and Geophysical Research Center, New Mexico Institute of Mining and Technology, Socorro, NM
(6) Department of Geological Sciences, University of Texas at Austin, TX
(7) Department of Physics, New Mexico State, Las Cruces, NM

Supplemental Information

Convection modeling for the Colorado Plateau margins

The numerical code CitCom (Moresi and Gurnis, 1996; Zhong et al., 2000) was used for the model calculations. We used a visco-plastic rheology, which combines linear, temperature and pressure dependent viscous Arrhenius type rheology for diffusion creep with activation energy E*=360 kJ/mole and activation volume V*=5 cm^3/mole with a pseudo-plastic rheology for Byerlee's law using a frictional coefficient of 0.7. The reference viscosity at reference mantle temperature T_m (1350°C) and reference depth z_r=660 km was $\eta_0 = 1.76 \cdot 10^{21}$ Pa·s. We further used thermal expansion $\alpha=3.5 \cdot 10^{-5}$ K^{-1}, diffusivity $K=1 \cdot 10^{-6}$ $m^2 s^{-1}$, specific heat c_p= 1250 $J \cdot kg^{-1} \cdot K^{-1}$, $\rho = 3300$ kg/m^3 and g=9.8 m/s^2. Model parameter values are adopted from van Hunen and Zhong (2003); only E^* and V* are taken from Karato and Wu (1993). E* controls thermal boundary layer instabilities (Davaille and Jaupart, 1994).
Thermal boundary conditions are 0°C at the free surface, 1350°C at the bottom of the model domain, and zero diffusive heat flux at side boundaries. The step in lithosphere thickness between the BRP and CP is included as an initial setup condition (see Fig. DR1). We also included ongoing extension in the BRP during the past 12 My as far-field

velocity boundary conditions imposed on the side boundaries. In tests in which the extension velocity was 0 mm/yr, the lithosphere below the BRP cools and thickens, and the step in lithosphere thickness between the CP and the adjacent regions decreases rapidly over time.
Tests are shown that were performed with a ~1580 km wide, 660 km deep model domain, covered by a grid of 97 vertical and 257 horizontal nodes. Varied parameters included the step in lithosphere thickness (the CP thickness of 140 km was held constant between tests; the initial BRP thickness was varied between 50 and 120 km, Fig. DR1), the BRP extension rate (between 0 and 10 mm/yr, shown are results with 6 mm/yr extension rate), and E* (the activation energy, which was varied between the standard value of 360 kJ/mol and a reduced value of 180 kJ/mol to mimic dislocation creep effects, Christensen, 1984; van Hunen et al., 2005). In addition we performed several tests with stress dependent rheology (with power law exponent 3.5) that however did not produce any significantly different results and hence are not further described here.
All asthenosphere-lithosphere boundary topographies tested were large enough to induce convection (Fig. 2). Such convective instabilities develop preferably near lithosphere inhomogeneities (Sleep, 2007). As expected for edge-driven convection, the convection cell that develops has upward flow of asthenosphere beneath the thinned areas of the BRP. Below the CP interior, a cold downwelling develops (Fig. 2). The tests differ in the temperature of this downwelling; the instability is between ~100 and ~250°C colder at 250 km depth than surrounding asthenosphere. The tests also differ in the lithosphere thickness of the BRP (tests with an initially thicker BRP lithosphere maintain a thicker lithosphere during the model evolution and vice versa), and hence, the BRP-CP temperature difference.

In modeling, the solidus (Fig. 2A) is crossed below the BRP and below the CP edge. The exact amount of modeled melt depends on the initial thickness of the BRP lithosphere, the extension rate, and the amount of convectively removed mantle lithosphere.

Synthetic seismic wave velocities
We calculated seismic wave velocities corresponding to the model temperature structures (Fig. 2, Fig. DR2). Seismic wave velocities were predicted from model temperatures including elastic and anelastic effects and variations of mineral phase composition with pressure and temperature, using the method described in Cobden et al. (2008), and van Wijk et al. (2008), and parameters listed in Tables DR1 and DR2. The expression for Q is $Q_S(T,z) = Q_0 \cdot \omega^a \cdot \exp(agT_m(z)/T)$. We use the parameters in Table DR2, which give a temperature-dependence similar to model "Q1" that provided compatible temperature estimates for V_P and V_S at lithospheric depths (Goes et al., 2000), but use the parameterization in terms of melting temperature to account for the pressure dependence. This Q model does quite well at reproducing the average velocity-depth gradients beneath the study region (Fig. 2, DR2, Van Wijk et al., 2008) down to about 250 km, but deeper gradients are somewhat lower than those found seismically. Other Q parameters may be able to also reproduce the deeper gradients (Faul and Jackson, 2005), or compositional heterogeneity may be required (Cammarano and Romanowicz, 2007, Cobden et al., 2008). The seismic conversion method has been tested, updated, and applied to the evaluation of lithosphere-upper-mantle structure and dynamics in a number of previous

studies (Goes et al., 2000, Goes and Van der Lee 2002, Cammarano et al., 2003, Cobden et al., 2008, Van Wijk et al., 2008; Hieronymus & Goes, 2010).

Seismic anomalies are relative to the model horizontal average, i.e., a regional reference, as in the tomography of Sine et al. (2008). The maximum, thermally induced, V_S contrast between CP and BRP lithosphere is about 12% for a constant pyrolitic composition (Fig. DR2). Other compositions were tested (e.g., a mechanical basalt-harzburgite mixture, Xu et al., 2008); they give quite different absolute velocities but hardly change the pattern and amplitude of the relative regional anomalies. Compositional differences alone between the CP lithosphere and BRP asthenosphere can enhance the velocity contrasts by a maximum of 1.5-2%, assuming an extremely depleted (dunitic) composition for all regions with temperatures less than 1200°C. A dunitic composition is an end member; it is more depleted than the available CP xenoliths, but has been suggested to be representative for old buoyant (Archean) lithosphere (e.g., Griffin et al. 2008), and produces the most extreme seismic velocity contrast.

Table DR1. Compositions in oxides in mole %

Composition	MgO	FeO	CaO	Al_2O3	SiO2	Reference
Pyrolite	48.53	5.72	3.50	1.80	38.66	*Sun*, 1982
Harzburgite	57.42	5.44	0.44	0.48	36.22	*Irifune & Ringwood*, 1987
Eclogite	16.31	6.70	14.58	9.88	52.54	*Perrillat, et al.*, 2006
Dunite	59.95	4.77	0.073	0.144	35.06	*Griffin et al.*, 2008

Table DR2. Anelasticity model

depth	Q0	a	ω	g	Q_K
0 km – ol-wad	0.1	0.15	0.02 Hz	40	1000
ol-wad – 660 km	0.5	0.15	0.02 Hz	30	1000

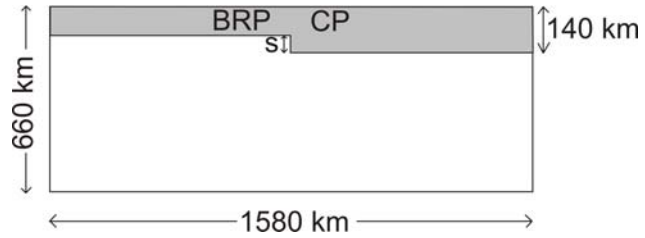

Figure DR1. Initial model setup, grey area denotes high viscosity lithosphere. The initial lithosphere thickness of the Colorado Plateau (CP) is 140 km in all tests; the lithosphere thickness of the Basin and Range Province (BRP) is varied between different tests. Therefore S, the step in lithosphere thickness between CP and BRP, varies between different tests.

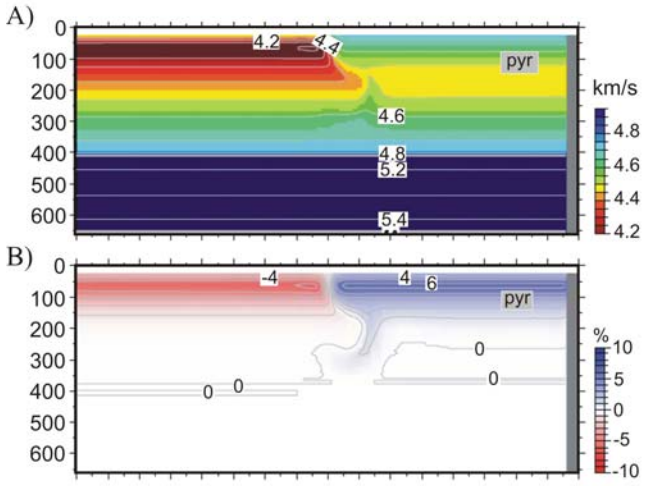

Figure DR2. S-wave seismic velocities and anomalies predicted by our models as described in the text, for a constant pyrolitic composition. A) Absolute S-wave velocities corresponding to temperatures in Fig. 2B. B) S-wave velocity anomalies relative to the layer average for structure in DR2A.

References

Cammarano, F., and Romanowicz, B., 2007, Insights into the nature of the transition zone from physically constrained inversion of long-period seismic data: Proceedings of the National Academy of Sciences of the United States of America, v. 104, p. 9139-9144.

Cammarano, F., Goes, S., and Vacher, P., 2003, Inferring upper-mantle temperatures from seismic velocities: Physics of the Earth and Planetary Interiors, v. 138, p. 197-222.

Christensen, U., 1984, Convection with pressure-dependent and temperature-dependent non-Newtonian rheology, Geophysical Journal Royal Astronomical Society, v. 77, 343-384.

Cobden, L.J., Goes, S., Cammarano, F., and Connolly, J.A.D., 2008, Thermo-chemical interpretation of one-dimensional seismic reference models for the upper mantle: evidence for bias due to heterogeneity, Geophysical Journal International, v. 175, p. 627-648.

Davaille, A., and Jaupart, C., 1994, Onset of thermal convection in fluids with temperature-dependent viscosity: application to the oceanic mantle: Journal of Geophysical Research, v. 99, p. 19853-19866.

Faul, U.H., and Jackson, I., 2005, The seismological signature of temperature and grain size variations in the upper mantle: Earth and Planetary Science Letters, v. 234, p.119-134.

Goes, S., Govers, R., and Vacher, P., 2000, Shallow mantle temperatures under Europe from P and S wave tomography: Journal of Geophysical Research, v. 105, 11153-11169.

Goes, S. and Van der Lee, S., 2002, Thermal structure of the North American uppermost mantle inferred from seismic tomography, Journal of Geophysical Research, v. 107, doi:10.1029/2000JB000049.

Griffin, W.L., O'Reilly, S.Y., Afonso, J.C., and Begg, G.C., 2008, The composition and evolution of lithospheric mantle: A re-evaluation and its tectonic implications: Journal of Petrology, doi:10.1093/petrology/egn033.

Hieronymus, C.F., Goes, S., 2010, Complex cratonic seismic structure from thermal models of the lithosphere: Effects of variations in deep radiogenic heating, Geophysical Journal International, in press.

Irifune, T., and Ringwood, A.E., 1987, Phase-transformations in a Harzburgite composition to 26 Gpa - implications for dynamical behavior of the subducting slab: Earth and Planetary Science Letters, v. 86, p. 365-376.

Karato, S., and Wu, P., 1993, Rheology of the upper mantle: a synthesis: Science, v. 260, p. 771-778.

Perrillat, J. P., Ricolleau, A., Daniel, I., Fiquet, G., Mezouar, M., Guignot, N., and Cardon, H., 2006, Phase transformations of subducted basaltic crust in the upmost lower mantle: Physics of the Earth and Planetary Interiors, v.157, p.139-149.

Sleep, N., 2007, Edge-modulated stagnant lid convection and volcanic passive margins: Geochemistry, Geophysics, Geosystems, v. 8, doi:10.1029/2007GC001672.

Sun, S.S., 1982, Chemical-Composition and Origin of the Earths Primitive Mantle: Geochimica Et Cosmochimica Acta, v. 46, p. 179-192.

van Hunen, J., and Zhong, S., 2003, New insight in the Hawaiian plume swell dynamics from scaling laws, Geophysical Research Letters, v. 30, 1785, doi:10.1029/2003GL017646.

Xu, W., Lithgow-Bertelloni, C., Stixrude, L., and Ritsema, J., 2008, The effect of bulk composition and temperature on mantle seismic structure: Earth and Planetary Science Letters, v. 275, p. 70-79.

Zhong, S., Zuber, M. T., Moresi, L., and Gurnis, M, 2000, Role of temperature-dependent viscosity and surface plates in spherical shell models of mantle convection. Journal of Geophysical Research, v. 105, 11063-11082.